Bioconjugate Chemistry

Article

pubs.acs.org/bc

Exploration of the Design Principles of a Cell-Penetrating Bicylic Peptide Scaffold

Rike Wallbrecher,[†] Luc Depré,[†] Wouter P. R. Verdurmen,[†] Petra H. Bovée-Geurts,[†] Richard H. van Duinkerken,[‡] Mariët J. Zekveld,[‡] Peter Timmerman,*[,‡] and Roland Brock*[,†]

[†]Department of Biochemistry (286), Radboud Institute for Molecular Life Sciences, Radboud University Medical Centre, Geert Grooteplein 28, 6525 GA Nijmegen, The Netherlands

[‡]Pepscan Therapeutics, Zuidersluisweg 2, 8243 RC Lelystad, The Netherlands

Supporting Information

ABSTRACT: Cell-penetrating peptides (CPPs) possess the capacity to induce cell entry of themselves and attached molecular cargo, either by endocytosis or by direct translocation. Conformational constraints have been described as one means to increase the activity of CPPs, especially for direct crossing of the plasma membrane. Here, we explored the structure−activity relationship of bicyclic peptides for cell entry. These peptides may be considered minimal analogues of naturally occurring oligocyclic peptide toxins and are a promising scaffold for the design of bioactive molecules. Increasing numbers of arginine residues that are primarily contributing to cell-penetrating activity were introduced either into the cycles, or as stretches outside the cycles, at both ends or at one end only. In addition, we probed for the impact of negatively charged residues on activity for both patterns of arginine substitution. Uptake was investigated in HeLa cells by flow cytometry and confocal microscopy. Overall, uptake efficiency showed a positive correlation with the number of arginine residues. The subcellular distribution was indicative of endocytic uptake. One linear stretch of arginines coupled outside the bicycle was as effective in promoting uptake as substituting the same number of arginines inside the bicycles. However, the internally substituted analogues were more sensitive to the presence of negatively charged residues. For a given bicyclic peptide, uptake was more effective than for the linear counterpart. Introduction of histidine and tryptophans further increased uptake efficiency to comparable levels as that of nonaarginine despite the larger size of the bicyclic backbone. The results demonstrate that both arginine clustering and spatial constraints are uptake-promoting structural principles, an observation that gives freedom in the introduction of cell-penetrating capacity to structurally constrained scaffolds.

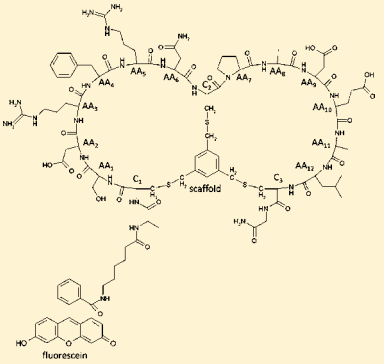

INTRODUCTION

Efficient cellular import is still a major hurdle in drug development. Many small molecules as well as biomacromolecules such as siRNA enter cells only poorly, thus requiring chemical modifications or carriers to induce cellular uptake. Over the past 20 years, there has been increasing interest in cell-penetrating peptides (CPPs) as carriers. These cationic or amphipathic peptides of about 8 to 30 amino acids in length can be coupled to drugs covalently or noncovalently.[1]

A high density of positive charge is a characteristic of the large majority of CPPs.[2] While for the amphipathic CPPs lysine residues frequently act as carriers of positive charge, the arginine-rich CPPs, as the name already suggests, possess a high density of arginine side chains. Prominent examples for the latter are the Tat peptide derived from the HIV transactivating protein[3] and the oligoarginines.[4,5] The particular role of arginines has been ascribed to the capacity of the guanidinium group to engage in bidentate hydrogen bond interactions, for example, with negatively charged sugars on the plasma membrane.[6]

For most CPPs and CPP−cargo complexes uptake occurs via endocytosis. This uptake mechanism requires endosomal escape in order to achieve delivery to the cytosol. However, next to endocytosis, CPPs can also enter via different mechanisms of direct membrane permeation. At low peptide concentrations, there is evidence for direct translocation across the plasma membrane,[7] while at high concentrations arginine-rich CPPs induce an activation of acid sphingomyelinase followed by rapid cytoplasmic entry via ceramide-rich membrane platforms, also coined nucleation zones.[8] This latter uptake mechanism has also been referred to as transduction.[9]

It has been proposed that interactions of CPPs with negatively charged heparan sulfate (HS) proteoglycans of the glycocalyx play a key role in triggering uptake.[10−14] However, overall the role of HS is not clear, as cells that are poor in HS expression such as Jurkat cells also show efficient uptake of CPPs.[1S,16]

Structural variants of the linear peptide backbone have always played an important role in CPP research, both in investigating the mechanisms of peptide uptake as well as in the

Received: March 14, 2014
Revised: April 3, 2014
Published: April 3, 2014

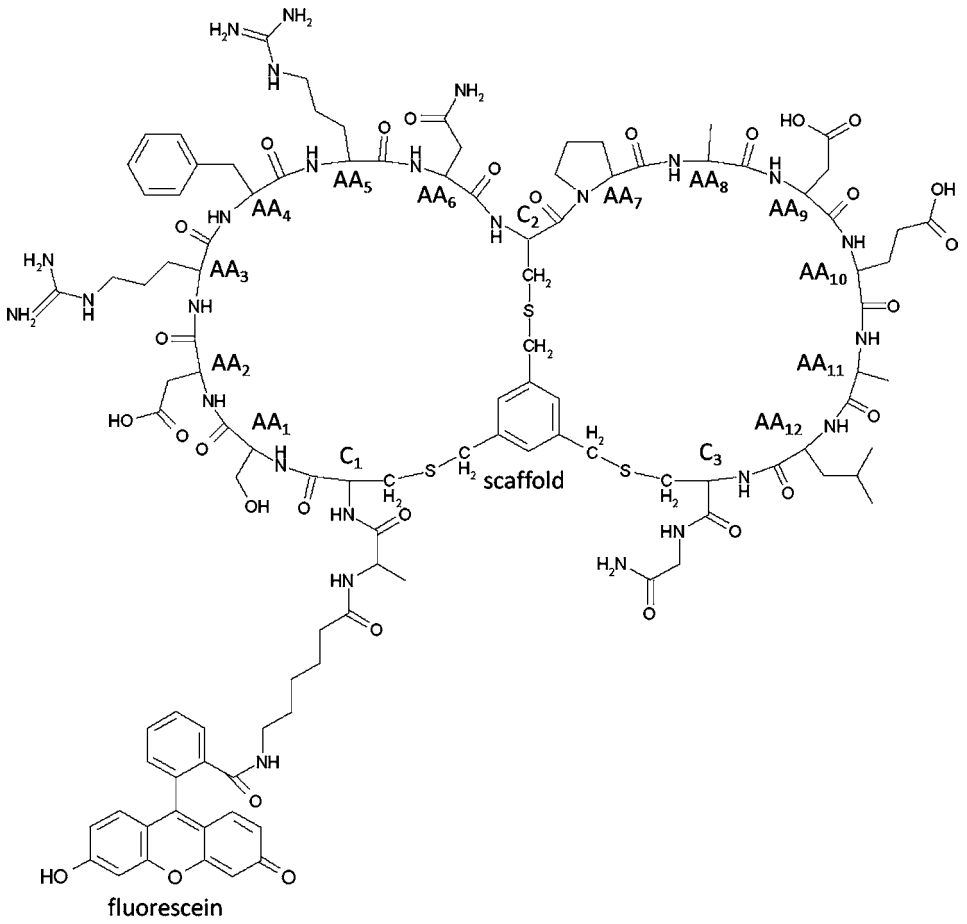

Figure 1. General structure of the bicyclic CPPs used in this study.

development of vectors with specific uptake characteristics and activity. For analogues of arginine-rich CPPs the role of structural flexibility has been scrutinized. Wender et al. showed that besides the number of arginine residues a longer and flexible spacer between the guanidino group and the peptide backbone improved uptake, indicating that structural flexibility of peptides is yet another important factor for internalization.[17] In contrast, it was also shown that cyclization of oligoarginines increased uptake by transduction.[18] This observation was ascribed to the increased conformational rigidity of the cyclic molecule and a longer spacing between the guanidino groups. For a CPP derived from the human milk protein lactoferrin, uptake also depends on the presence of a disulfide bond formed by terminal residues.[10] However, in this case this observation can be attributed to the generation of a higher local arginine density.[14] Notably, also the entry mechanism of several oligocyclic peptide toxins that exert their activity inside the cell bears similarities with the one of CPPs. Examples are maurocalcine[19] and crotamine.[20] For maurocalcine, current evidence supports endocytosis subsequent to HS binding as the mechanism of uptake, even though the molecular target resides on the cytosolic face of the membrane of the endoplasmic reticulum.[21]

Overall, constraining an oligopeptide into a polycycle represents a highly interesting principle for the generation of conformationally constrained, compact molecules which are less prone to enzymatic degradation. However, the formation of a defined array of multiple disulfide bonds, which are most frequently used for cyclization, can be synthetically challenging. Using tris (bromomethyl)benzenes, bicyclic molecules can be synthesized from peptides bearing three cysteine residues using straightforward chemistry.[22] Here, we employed this "CLIPS"-chemistry (Chemical LInkage of Peptides to Scaffolds) to investigate the structure−activity relationship of arginine-substituted bicyclic peptides with respect to uptake efficiency and mechanism. Arginine residues were either placed in the cyclic parts of the molecule or attached to the N- or C-terminal ends outside the bicycle. Uptake efficiency and subcellular distribution were investigated by flow cytometry and confocal microscopy. Furthermore, the impact of cyclization on uptake was assessed for a subset of bicycles and the interaction with HS studied using isothermal titration calorimetry. Finally, we investigated whether the incorporation of histidine and tryptophan residues next to arginines had an impact on endosomal escape. The design principles elucidated here will guide the implementation of cell-penetrating capacity into such types of constrained bioactive molecules.

RESULTS

Design of the Bicyclic Peptides. All bicyclic peptides were based on a core structure of three cysteine residues into which two six-amino-acid loop segments of glycine and serine residues were introduced (Figure 1). The N-terminus was extended with an alanine and an aminohexanoic acid spacer to attach the carboxyfluorescein moiety needed to follow cellular uptake by flow cytometry and confocal microscopy. A glycine residue was added at the C-terminal end (Table 1).

dx.doi.org/10.1021/bc500107f | Bioconjugate Chem. 2014, 25, 955−964

Table 1. Sequences of the Bicyclic Peptides Used in This Study

name	group	peptide sequence	total charge
IA0	Internal arginine	FITC-Ahx-ACSGSGSGCGSGSGSCG[a]	0
IA2		FITC-Ahx-ACSG**R**GSGCGSG**R**GSCG[a,b]	+2
IA4a		FITC-Ahx-AC**R**GSG**R**GCG**R**GSG**R**CG[a]	+4
IA4b		FITC-Ahx-ACSG**R**G**R**GCG**R**G**R**GSCG[a]	+4
IA6a		FITC-Ahx-AC**R**G**R**G**R**GCG**R**G**R**G**R**CG[a]	+6
IA6b		FITC-Ahx-ACG**R**G**R**G**R**CG**R**G**R**G**R**GCG[a]	+6
IA6c		FITC-Ahx-AC**R**G**R**G**R**GCG**R**G**R**G**R**GCG[a]	+6
IA6d		FITC-Ahx-ACG**R**G**R**G**R**CG**R**G**R**G**R**CG[a]	+6
IA8a		FITC-Ahx-AC**R**G**RRR**GCG**RRR**G**R**CG[a]	+8
IA8b		FITC-Ahx-AC**RR**S**RR**GCG**RR**S**RR**CG[a]	+8
kCA2	Kallikrein inhibitor with internal arginines	FITC-Ahx-ACS<u>D</u>**R**F**R**NCPA<u>DE</u>ALCG[a]	−1
kCA3		FITC-Ahx-AC**R**<u>D</u>**R**F**R**NCPA<u>DE</u>ALCG[a]	0
kCA4		FITC-Ahx-AC**R**<u>D</u>**R**F**R**NCPA<u>DE</u>**R**LCG[a]	+1
kCA5		FITC-Ahx-AC**R**<u>D</u>**R**F**RR**CPA<u>DE</u>**R**LCG[a]	+2
kCA6		FITC-Ahx-AC**R**<u>D</u>**R**F**RR**CPA<u>D</u>**RR**LCG[a]	+4
CA2	Control internal arginine	FITC-Ahx-ACSG**R**G**R**GCGSGSGSCG[a]	+2
CA3		FITC-Ahx-AC**R**G**R**G**R**GCGSGSGSCG[a]	+3
CA4		FITC-Ahx-AC**R**G**R**G**R**GCGSGS**R**SCG[a]	+4
CA5		FITC-Ahx-AC**R**G**R**G**RR**CGSGS**R**SCG[a]	+5
CA6		FITC-Ahx-AC**R**G**R**G**RR**CGSG**RR**SCG[a]	+6
EA2x1	External arginines	FITC-Ahx-A**R**CSGSGSGCGSGSGSCG**R**[a]	+2
EA2x2		FITC-Ahx-A**RR**CSGSGSGCGSGSGSCG**RR**[a]	+4
EA2x3		FITC-Ahx-A**RRR**CSGSGSGCGSGSGSCG**RRR**[a]	+6
EA2x4		FITC-Ahx-A**RRRR**CSGSGSGCGSGSGSCG**RRRR**[a]	+8
EA1x8		FITC-Ahx-ACSGSGSGCGSGSGSCG**RRRRRRRR**[a]	+8
kEA2x1	Kallikrein inhibitor with external arginines	FITC-Ahx-A**R**CS<u>D</u>**R**F**R**NCPA<u>DE</u>ALCG**R**[a]	+1
kEA2x2		FITC-Ahx-A**RR**CS<u>D</u>**R**F**R**NCPA<u>DE</u>ALCG**RR**[a]	+3
kEA2x3		FITC-Ahx-A**RRR**CS<u>D</u>**R**F**R**NCPA<u>DE</u>ALCG**RRR**[a]	+5
kEA2x4		FITC-Ahx-A**RRRR**CS<u>D</u>**R**F**R**NCPA<u>DE</u>ALCG**RRRR**[a]	+7
kEA1 × 8		FITC-Ahx-ACS<u>D</u>**R**F**R**NCPA<u>DE</u>ALCG**RRRRRRRR**[a]	+7
IA8b L	Linear variants	FITC-Ahx-AC**RR**S**RR**GCG**RR**S**RR**CG[d]	+8
CA6 L		FITC-Ahx-AC**R**G**R**G**RR**CGSG**RR**SCG[d]	+6
EA1x8 L		FITC-Ahx-ACSGSGSGCGSGSGSCG**RRRRRRRR**[d]	+8
kEA1x8L		FITC-Ahx-ACS<u>D</u>**R**F**R**NCPA<u>DE</u>ALCG**RRRRRRRR**[d]	+7
EA8_4H	Histidine/tryptophan peptides	FITC-Ahx-ACSHSGHGCGHGSHSCG**RRRRRRRR**[a]	+8
EA8_2H2W		FITC-Ahx-ACSHSGWGCGHGSWSCG**RRRRRRRR**[a]	+8
IA5_2H1W		FITC-Ahx-ACHG**RR**WGCG**R**HRGRCG[a]	+5

[a]All cysteines form disulfide bridges with the T3-scaffold. [b]Arginine is highlighted in bold, negative charges are underlined. The N-termini are labeled with FITC and the C-termini are amidated. [c]kCA2 is identical to the high-affinity kallikrein inhibitor reported by Heinis and Winter.[23] [d]All cysteines were capped with iodoacetamide.

Increasing numbers of arginine residues, to a maximum of eight, were introduced either into the cycles in replacement for serine residues (IA group) or attached outside the cycles to either one (C-terminus) or both ends of the bicyclic peptide (EA group) (Table 1). In order to explore whether a specific structural arrangement of arginines in the cycles also had an influence on activity, several analogues with the same number of arginines but at different positions were synthesized. Since the ultimate goal would be to achieve cell penetration for a bioactive molecule, we also introduced arginines into a bicycle that had been identified as an inhibitor of the human plasma kallikrein protease[23] by phage display library screening. Since this peptide (kCA2) contained negatively charged aspartate and glutamate residues, we wanted to learn to what extent the presence of negatively charged residues was compatible with uptake. To address the impact of cyclization on uptake, we also synthesized several linear analogues. A final group was composed of analogues in which histidine and tryptophan residues were introduced next to arginines to investigate whether their presence had an impact on uptake and endosomal release.

Cellular Uptake of Bicyclic Peptides. First, uptake of peptides with internal arginines (IA) was tested by flow cytometry, at both 5 and 20 μM. These concentrations were selected because for arginine-rich peptides at 5 μM uptake typically occurs via endocytosis, while at 20 μM rapid

dx.doi.org/10.1021/bc500107f | Bioconjugate Chem. 2014, 25, 955−964

cytoplasmic import is observed.[24] Also, cells showed this rapid uptake for cyclic deca-arginine at 15 μM using serum-free conditions.[18]

At 5 μM, the uptake efficiency of the tested bicyclic peptides showed a positive correlation with the number of arginines (Figure 2A–C). For the analogue with two and four arginines

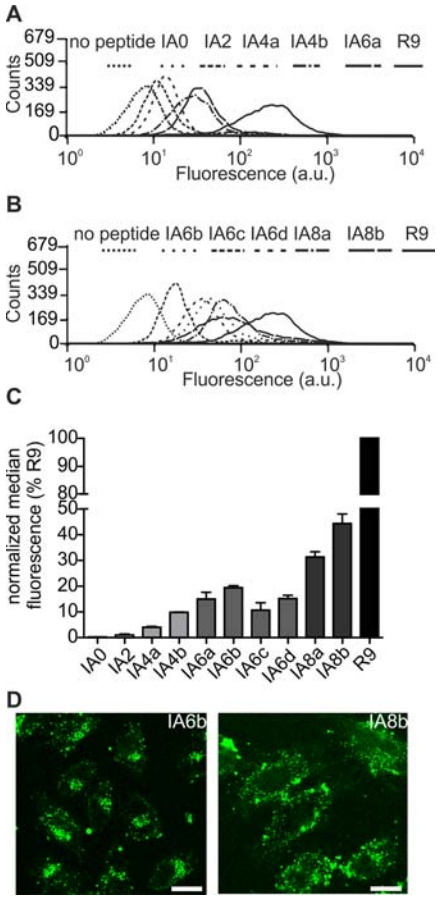

Figure 2. Structure–activity relationships of the bicyclic peptides with arginine substitutions within the cycles (IA group). (A,B) Flow cytometry histograms of bicycles and nonaarginine at 5 μM for HeLa cells after 1 h incubation with peptides. (C) Average median of at least 3 flow cytometry measurements and the standard error. All values were corrected for the background of cells incubated without peptides. (D) Intracellular distribution of the indicated peptides at 5 μM determined by confocal microscopy. The same settings were used for image acquisition of both peptides. Scale bar represents 20 μm.

(IA2 and IA4a-b), uptake was less than 10% of that of nonaarginine. Interestingly, for the set of analogues with six arginine residues (IA6a-d), only IA6b, in which the arginine residues were positioned at every other position, was taken up significantly better than the peptides with fewer arginine residues (SI Table 1). The uptake efficiency further increased by introducing two more arginine residues, with the peptide having the regularly distributed arginine pairs (IA8b) showing the highest uptake. However, even for this most efficient bicycle, uptake was only about 45% of the import of nonaarginine, which was used as a reference.

At 20 μM the uptake differences were similar to those at 5 μM (SI Figure 2). There were no differences between the peptides with six and eight arginines, though. In addition, the most efficient peptides displayed only 20% of the uptake of nonaarginine. The flow cytometry histograms showed no indications of rapid cytoplasmic import which either constitutes itself as a strong rightward shift of the histogram or by the presence of a second population.

Confocal laser scanning microscopy demonstrated that fluorescence was present in punctate structures at 5 μM indicating that the bicycles are taken up by endocytosis (Figure 2D, SI Figure 1). For microscopy, we focused on the concentration of 5 μM, because flow cytometry had not shown any evidence of a concentration-dependent change in uptake mechanism.

Next, we assessed the impact of negatively charged amino acids on the import efficiency by introducing arginine substitutions into the kallikrein inhibitor peptide[23] (CA group). The positioning of arginines deviated from that of the first set in order to avoid substitution of residues specific for the inhibitor. Arginines were placed into a bicycle either without the negatively charged residues present in the kallikrein inhibitor (CA group) or into the kallikrein inhibitor $AC_{T3}SDRFRNC_{T3}PADEALC_{T3}G$ that contains three negatively charged residues (kCA group). kCA2 ($AC_{T3}SDRFRNC_{T3}PADEALC_{T3}G$) is identical to the bicycle having the highest affinity for the kallikrein protease.[23] For the CA group, uptake was lower than for the IA group, but this needs to be attributed primarily to the fact that these bicycles carried a lower number of positive charges (SI Figure 3). For arginine-substituted variants of the kallikrein-derived peptides (kCA), uptake was even lower than for the respective control peptides (CA), demonstrating that the presence of negatively charged residues in close proximity to arginine residues compromised uptake (SI Figure 3).

After having explored the impact of arginine substitutions within the bicycles, we were interested in the activity of bicycles for which arginines were attached externally (EA group). In this way, the design of these molecules followed the more classical approach where a cell-penetrating moiety is attached to a cargo molecule. At the same time, the arginine residues are not subject to conformational constraints any more. Oligoarginines were attached to both ends of the bicycle at the same time, or only to the C-terminus. The kallikrein inhibitor was also included to assess the impact of the presence of negative charge in this structural arrangement (kEA group).

Again, uptake efficiency correlated positively with the number of arginines (Figure 3). When a stretch of eight arginines was added at the C-terminus (EA8), the uptake was twice as high compared to two stretches of four arginines at both termini (EA2x4) (for statistics see SI Table 2). Here, the negative charge of the kallikrein inhibitor had no effect on uptake, which stands in sharp contrast to what was observed for the internally substituted bicycles; uptake for the analogue extended by an octaarginine (kEA8) and having the kallikrein inhibitor motif was in the same range as uptake for the bicycle that carried eight external arginine substitutions (EA8). Confocal microscopy experiments revealed mainly endosomal staining (SI Figure 4). Cytoplasmic staining was also visible for peptides EA1x8 and kEA1x8 (Figure 3D).

Comparison of Bicyclic with Linear Variants. Characterization of the bicycles indicated that an external octaarginine stretch promoted uptake as effectively as the same number of arginines within the conformationally constrained bicycle. To evaluate whether cyclization contributed to activity of these bicycles or whether activity was a function of the arrangement

dx.doi.org/10.1021/bc500107f | Bioconjugate Chem. 2014, 25, 955–964

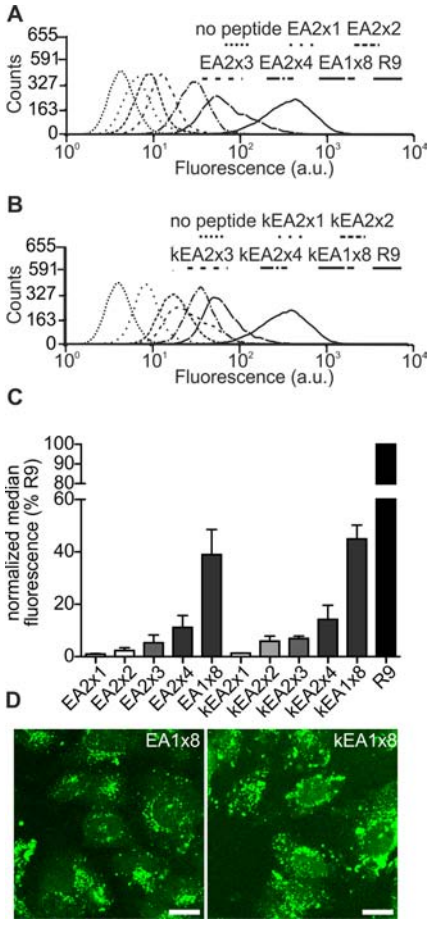

Figure 3. Structure–activity relationship of the bicyclic peptides with external oligoarginine elongations (EA group). (A,B) Flow cytometry histograms of bicycles and nonaarginine at 5 μM for HeLa cells after 1 h incubation with peptides. (C) Average median of at least two flow cytometry measurements and the standard error. (D) Subcellular distributions of the bicyclic peptide EA1x8 and kEA1x8 at 5 μM measured by confocal microscopy. The same settings were used for image acquisition of both peptides. Scale bar represents 20 μm.

of arginines in the primary peptide structure, bicyclic variants were tested next to their linear counterparts (Table 1).

Two bicycles with internal substitutions (IA8b, CA6) and two C-terminally extended bicycles with/without the kallikrein sequence ((k)EA1x8) were included. We restricted our analysis to 5 μM peptide concentrations, as before no concentration dependence was observed in the uptake experiments. In all cases, uptake of the bicyclic variants was more effective than uptake of the linear ones (Figure 4) (for statistics, see SI Table 3). Except for differences in uptake efficiency, confocal microscopy did not reveal remarkable differences in subcellular localization of the peptides.

Next to assessing uptake efficiency after short-term incubation (1 h), we were also interested in determining whether cyclization conferred an advantage over longer incubation times of 18 h. In 10% fetal calf serum, nonaarginine is degraded with a half-life of about 1 h.[25] Cyclization should protect the peptides against proteolytic breakdown, thereby increasing the cell-associated fluorescence in comparison to the linear counterparts. Furthermore, we were also interested to learn whether fluorescence was still punctate or whether a more pronounced release into the cytosol would occur. In this analysis, we also included one bicycle with six internal arginine substitutions (CA6) to determine whether the potential stabilization to proteolysis over longer incubation times would compensate for less efficient uptake over short incubation times.

For most peptides, the cell-associated fluorescence was lower after 18 h compared to 1 h, which is indicative of proteolytic breakdown followed by release of fluorescein[26] (Figure 4). However, for all except one peptide (CA6), this drop in fluorescence was lower for the cyclic variant than for the linear counterpart (Figure 5) (for statistics see SI Table 4). This result demonstrates that the spatial constraint also conferred an advantage for long-term activity which is probably due to proteolytic stability.[26] Overall, the remaining cell-associated fluorescence was higher for the peptides with lower charge (CA6). This may be explained either by the fact that these peptides entered cells more slowly and were therefore longer protected against proteolytic degradation or by a preferential cleavage next to arginine residues. However, after 18 h the punctate subcellular distribution of fluorescence was even more pronounced than after 1 h, indicating that only those peptides that had been sequestered in endolysomal structures were retained, while cytoplasmic fluorescence was released.

Stability of Different Classes of Bicyclic Peptides. The external elongation with arginines proved to be as efficient in promoting uptake as the substitution with the same number of arginines within the bicycles. However, oligoarginines are known to serve as substrates for the furin protease.[27,28] To obtain a direct experimental validation for the differences in proteolytic stability, the degradation of two bicyclic peptides was followed in serum over time (Figure 6). In human serum the externally elongated peptide kEA1x8 was less stable than IA6b. The half-life of kEA1x8 was approximately 30 min and the half-life of IA6b was more than 1 h. The control incubation of the peptides in PBS showed no breakdown of the peptide or loss of fluorescence.

Interaction of Bicyclic and Linear Peptides with Heparan Sulfate (HS). Previously, we had investigated the thermodynamics of the interaction of linear nonaarginine with HS using isothermal titration calorimetry.[15] Even though the role of HS in the induction of peptide uptake is still under debate,[16] these negatively charged oligosaccharides interact with arginine-rich CPPs at the cell surface.[12] In particular, we were interested to learn whether cyclization affected the entropic changes related to peptide binding. Next to EA2x4 (with both C- and N-terminal tetra-arginines), the internally substituted IA8b bicyclic peptide (with eight arginines) was selected.

The bicyclic IA8b had a dissociation constant of 0.18 μM which is very similar to the one determined for nonaarginine previously[15] (Table 2). Interestingly, the dissociation constant of the peptide with the two external tetraarginines (EA2x4) for HS was more than twice as high as that for nonaarginine which is fully consistent with the lower uptake efficiency for EA2x4 as compared to IA8b. For both peptides, the enthalpy of the reaction and the entropy loss were on the same order of magnitude as for nonaarginine (Table 2, SI Figure 6).

Bicyclic Peptides with Histidine and Tryptophan Substitutions. After having shown that the bicyclic peptides were retained in the endosomes, we were aiming to promote the endosomal escape of these peptides by introducing histidine and/or tryptophan residues into the bicyclic peptides. Histidine and tryptophan were already shown to have a positive effect on

dx.doi.org/10.1021/bc500107f | Bioconjugate Chem. 2014, 25, 955–964

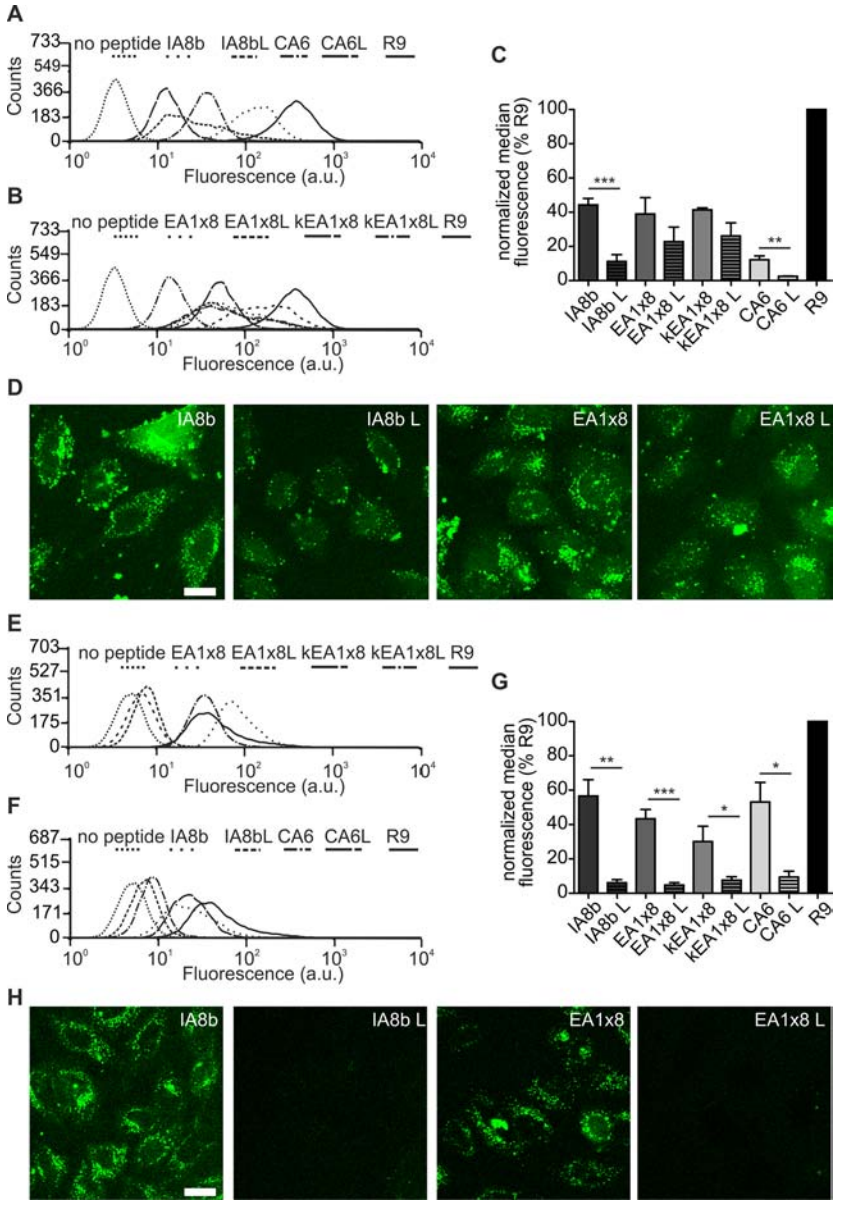

Figure 4. Uptake of selected bicyclic peptides and their corresponding linear variants after different incubation times. HeLa cells were incubated for 1 h (A–D) or 18 h (E–H) with 5 μM of the peptides at 37 °C. (A–B, E–F) Representative flow cytometry histograms. (C,G) Average median of five (C) or two (G) flow cytometry measurements and the standard error. All values were corrected for the background fluorescence (cells incubated without peptides) and medians of each experiment were normalized to nonaarginine (* indicates $p < 0.05$, ** $p < 0.001$, *** $p < 0.0001$). (D,H) Confocal microscopy images of the intracellular distribution of selected peptides. Different settings were used for image acquisition of peptides after 1 h (D) and 18 h incubation (H). Scale bar represents 20 μm.

endosomal escape. For histidine this has been assigned to the "proton sponge" effect of the imidazole ring leading to the rupture of the endosomes and/or with the capacity of the imidazole to interact with the endosomal membrane.[29−32] Moreover, tryptophan can destabilize the endosomal membranes by interacting and inserting into the lipid bilayer[33,34] and thereby promote endosomal rupture. We designed three bicyclic peptides (Table 1) based on IA5 and EA1x8, one containing four histidine residues (EA8_4H) and two bicycles containing both two histidine residues and either one (IA8_2H1W) or two tryptophan residues (EA8_2H2W). The peptides showed the same uptake efficiency as nonaarginine, being much higher than the uptake efficiencies of the corresponding peptides with only the external or internal arginine substitutions (Figure 7). However, the intracellular localization was comparable to that of other peptides (Figures 3D, 7C). Nevertheless, the data indicates that introduction of histidine and/or tryptophan had a clear added value on uptake efficiency.

DISCUSSION

Here, we explored the structure−activity relationship of cellular uptake for conformationally constrained bicyclic CLIPS-peptides.[22] In particular, we addressed the introduction of cell-penetrating capacity by substitutions inside the bicycles and by external elongations with arginines. All linear tricysteine peptides were synthesized using Fmoc-based solid-phase synthesis followed by the very efficient tandem ligation−cyclization reaction with tris(bromomethyl) benzene under high dilution conditions (100−500 μM) using the CLIPS

dx.doi.org/10.1021/bc500107f | Bioconjugate Chem. 2014, 25, 955−964

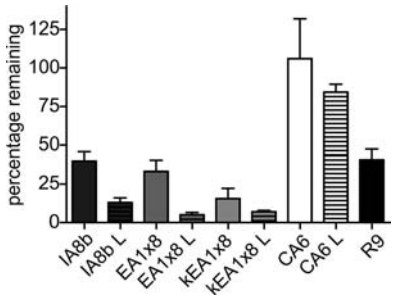

Figure 5. Cellular retention of fluorescence. The fluorescence intensity of the 18 h incubation was divided by that of the 1 h incubation (from the same experiment), represented by a percentage. The percentages of two experiments were averaged and plotted. Error bars show standard errors.

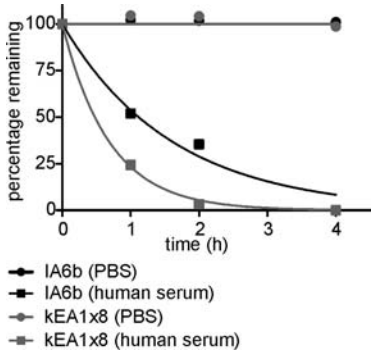

Figure 6. Proteolytic stability of IA6b and kEA1x8. The fraction of intact peptide was measured over time when incubated in 50% human serum (diluted with PBS) and in PBS. The SEM of three experiments was calculated for each condition and varied between 0.1% and 1%.

chemistry. The efficiency of these reactions is generally very high (>70%) but is slightly sequence-dependent. For the bicyclic peptides reported in this paper, the overall isolated yields (after preparative HPLC purification) ranged between 30% and 40%.

Through introduction of arginines, we were able to make the inhibitor for human kallikrein protease cell permeable. Overall, there was a positive correlation of import with the number of arginine residues. At least four arginine residues were required to achieve a significant import, both for internal arginine substitutions and for external elongation. Uptake of the bicycles was more efficient than that of their linear counterparts, which is consistent with previous data from experiments with arginine-rich peptides. It was shown that conformationally constraining oligoarginines through cyclization promoted uptake.[18] Furthermore, we had shown for a lactoferrin-derived CPP that cyclization through formation of a disulfide bridge enhanced the interaction with heparan sulfates through a local increase of arginine density.[10,14] Since the internally substituted

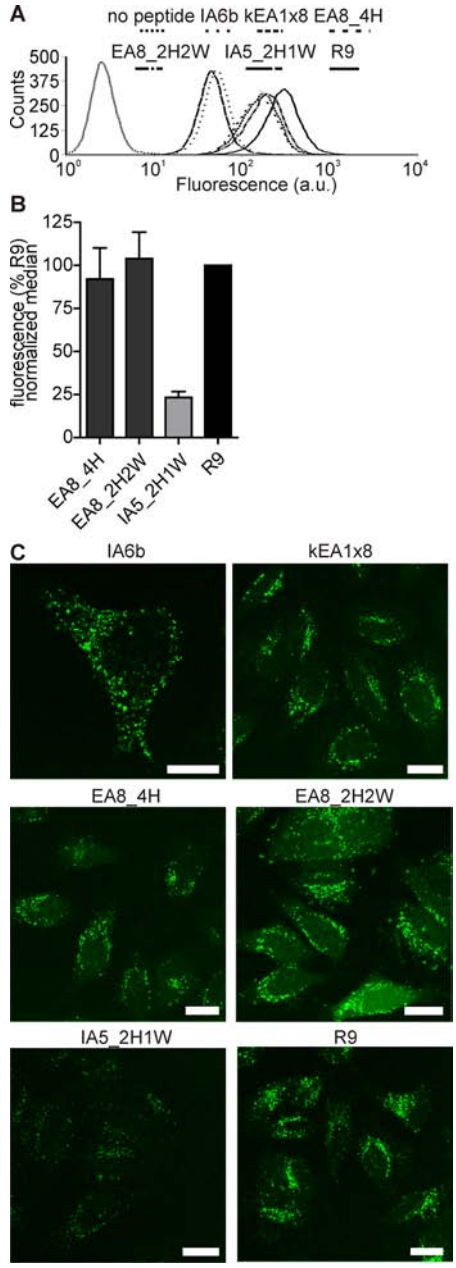

Figure 7. Uptake of bicyclic peptides, modified with histidine and tryptophan, and R9 in HeLa cells. HeLa cells were incubated for 1 h at 37 °C with 5 μM of the indicated peptides. (A) Flow cytometry histograms. (B) Average median of four flow cytometry measurements and the standard error. (C) Subcellular distribution of fluorescence was visualized by confocal microscopy. The same settings were used for image acquisition of all peptides. The scale bar denotes 20 μm.

Table 2. Properties of Binding of Bicyclic Peptides to HS

			enthalpy	entropy		
	N Sites/HS	K_D (μM)	ΔH kcal/mol	ΔS cal/(mol*deg)	ΔH/mol pep	ΔH/Arg
EA2x4 (n = 3)	12 ± 5[a]	0.45 ± 0.05	−64 ± 3	−180 ± 2	−6.6 ± 3	−0.82 ± 0.42
IA8b (n = 2)	14 ± 2	0.18 ± 0.09	−73 ± 4	−214 ± 14	−5.3 ± 1	−0.66 ± 0.13

[a]Values were obtained by measuring: enthalpy, stoichiometry, and affinity. Other properties were determined by using Gibbs free energy law. $\Delta G = -RT\ln$; $K_d = -\Delta H - T\Delta S$. Free energy ($\Delta G$) and entropy ($\Delta S$) were calculated with temperature (T) and gas constant (R).

dx.doi.org/10.1021/bc500107f | Bioconjugate Chem. 2014, 25, 955−964

bicycles had arginines introduced into a scaffold consisting of serines and glycines, the lactoferrin-derived peptide may be the more valid comparison.

The fact that the bicycles with the external arginines showed a more efficient uptake than their linear counterparts can be explained by the higher compactness in conjunction with a higher proteolytic stability afforded by cyclization. In addition, one consecutive stretch of arginine residues (EA1x8) was more active in inducing uptake than two external elongations, with each half the number of arginines (EA2x4) which demonstrates that local charge density is a decisive factor in inducing uptake. It is important to note that, despite the fact that the CLIPS−peptides are relatively large cargos, through the incorporation of arginine residues, we achieved an uptake efficiency that was up to 45% that of nonaarginine. The introduction of histidine and tryptophan residues into the arginine-rich bicycles further increased the uptake efficiencies to levels of nonaarginine. This is quite remarkable given the fact that the bicyclic scaffold, compared to nonaarginine, may be considered a large scaffold which may decrease the uptake efficiency.[35] These structural insights will be highly relevant for rendering bioactive, conformationally constrained peptides cell penetrating, especially when the pharmacophore contains histidine residues.

Interestingly, there were no indications of nucleation zone dependent import, also not at higher concentrations. Even though for some peptides fluorescence was also present in the cytosol, the major part of fluorescence was confined to punctate structures, strongly indicative of endocytic uptake. Therefore, there were also no indications that cyclization increased translocation efficiency, relating to a direct membrane permeation without activation of acid sphingomyelinase.[36] In contrast, nonaarginine[24] and its cyclic counterpart[18] showed highly efficient nucleation zone-dependent import. For the internally substituted peptides, this may be attributed to the fact that the induction of this import pathway, which provides direct access into the cytoplasm, critically depends on local arginine density. For the terminally substituted peptide this is consistent with the observation that this import route is compromised by cargo exceeding the size of a small peptide.[8,9]

Our results also illustrate the added value of a comparison of long over short incubation times for a deeper understanding of the impact of cyclization on import and intracellular sequestration. Nowadays, cells are typically incubated with CPPs for 30 min to 1 h only. This choice is primarily motivated by the fact that for longer incubation times the peptides distribute over intracellular compartments, and as a consequence, information on import routes is lost.[24] Also, elimination of peptide through proteolytic degradation may superimpose import.[26] However, as cyclization improved the proteolytic stability, testing of longer incubation times is particularly useful in determining the impact of this modification on long-term import capacity and intracellular retention. In fact, with one exception (CA6), bicyclic peptides showed a stronger intracellular retention over longer incubation times than their linear counterparts.

For two peptides we confirmed that the external elongation was more sensitive to proteolytic degradation than the internal substitution. However, although the externally substituted peptide was proteolytically less stable (kEA1x8) than the internally substituted one (IA6b), kEA1x8 was taken up more efficiently than IA6b. Overall the data indicate that a consecutive stretch of arginine residues has the strongest uptake promoting effect. However, the peptide with the internal substitution will better retain long-term activity due to a higher proteolytic stability.

Also, for one bicycle (CA6) that showed rather little uptake after 1 h, cell-associated fluorescence was about as high as that of the other peptides after the longer incubation time. This result also indicates that instead of selecting CPPs based on maximum activity during short-term incubation, for *in vivo* applications it would be desirable to select CPPs based on activity during long-term incubation, which may identify CPPs with fewer arginines and therefore reduced sequestration into the liver and kidney.[37,38]

For several CPPs, the requirement of HS for efficient cellular import has been reported.[39,40] Here, we showed that the affinities of two bicyclic peptides with the same number of arginines for HS varied by a factor of 2.5: the bicyclic peptide with eight internal arginines had a 2.5× higher affinity compared to the one with two external tetra-arginine stretches. This difference in HS affinity is in line with the more efficient uptake of the higher affinity peptide supporting the importance of HS for uptake of these bicyclic peptides. However, for both bicycles the thermodynamic parameters were in the same range as for nonaarginine, which demonstrates that cyclization did not afford an advantage in the entropy changes for HS-binding.

In conclusion, we successfully demonstrated the synthesis and cyclization of cell-penetrating bicyclic CLIPS−peptides by the introduction of arginine residues. The CLIPS architecture afforded peptides with long-term proteolytic stability that promoted uptake efficiency. In the future, the obtained insights will guide the introduction of cell-penetrating capacity into bioactive, conformationally constrained peptides.

■ EXPERIMENTAL PROCEDURES

Cell Culture. HeLa cells originally obtained from the American Type Culture Collection (Rockville, USA) were cultured in RPMI 1640 supplemented with 10% Fetal Calf Serum (FCS) (all from Gibco, Invitrogen, Eugene, USA). Cells were grown in an incubator at 37 °C with a humidified atmosphere and 5% CO_2 for 2 or 3 days before passaging.

Peptide Synthesis. All linear tricysteine peptides with an N-terminal carboxyfluorescein group were synthesized using standard Fmoc-based solid-phase peptide synthesis on a Rink-amide resin. The bicyclic peptides were then formed via a tandem ligation−cyclization reaction with equimolar amounts of tris(bromomethyl) benzene (1.05 equiv) in a mixture of ACN/H_2O 1:3 under high dilution conditions (typically at 100−500 μM) using ammonium bicarbonate as a base (pH ∼ 8.0). The efficiency of these reactions is generally very high (>70%) but varies slightly for different sequences. The overall isolated yields for the reported bicycles (after preperative HPLC purification) ranged between 30% and 40%.

For the synthesis of the linear variants of the bicycle peptides, we alkylated the linear tricysteine peptides with a slight excess (∼2 equiv) of iodoacetamide under the same reaction conditions as used for the cyclization reaction. The conversions were complete within 1 h and workup and purification of the peptides followed the same route as described for the bicyclic peptides. The concentrations of fluorescein-labeled peptides were determined by measuring the absorbance of fluorescein at 492 nm, assuming a molar extinction coefficient in 100 mM Tris-HCl pH 8.8 of 75 000 cm^{-1} M^{-1} on a Novaspec II visible spectrophotometer (Pharmacia/Pfizer, New York, USA).

Flow Cytometry. HeLa cells were seeded in a 24-well plate (Greiner Bio-One, Kremsmuenster, Austria) at a density of

80 000 cells per well 1 day or 40 000 cells per well 2 days before the experiment. Peptides were diluted to 5 or 20 μM depending on the experiment in phenol red-free RPMI containing 10% FCS. After washing the cells with Hepes-buffered saline (HBS; 10 mM HEPES, 135 mM NaCl, 5 mM KCl, 5 mM $MgCl_2$, 1.8 mM $CaCl_2$), 400 μL of the peptide solution was added per well. The peptides were incubated for 1 or 18 h at 37 °C followed by washing twice with HBS. For detachment and removal of surface-bound peptide, 300 μL trypsin (Pan Biotech, Aidenbach, Germany) was added and the cells were incubated for 5 min at 37 °C and washed by centrifugation (5 min, 1000 rpm). After resuspension in phenol red-free medium, internalized peptide was quantified with a FACS-Calibur Flow Cytometer (BD Biosciences, Erembodegem, Belgium) and gated for living cells based on forward versus sideward scatter. For each peptide condition at least 10 000 gated cells were measured and analyzed with the Summit software (Fort Collins, USA).

Confocal Microscopy. 40 000 HeLa cells per well were seeded in 8-well nunc chambers 1 day or 20 000 cells per well 2 days in advance of the experiment (Thermo Fisher Scientific, Rochester, USA). The peptides were diluted in phenol red-free RPMI + 10% FCS to 5 or 20 μM. After washing the cells with HBS, 200 μL of the solution containing the peptide was added per well. The cells were incubated for 1 or 18 h at 37 °C, washed twice with HBS, and finally 200 μL phenol red-free RPMI + 10% FCS were added per well. The cellular distribution of fluorescence was recorded using a TCS SP5 confocal microscope (Leica Microsystems, Mannheim, Germany) equipped with an HCX PL APO 63 × 1.2 N.A. water immersion lens at 37 °C. For excitation of fluorescein an argon ion laser was used (488 nm) and emission was collected between 500 and 550 nm.

Isothermal Titration Calorimetry (ITC). ITC experiments were performed with an ITC_{200} Microcal instrument (Microcal LLC, Wolverton Mill, UK). Peptide and HS (average molecular weight 13.6 kDa, Celsus Lab, Cincinnati USA) solutions were diluted in HBS to 30 μM and 90 μM, respectively. The sample cell was filled with the peptide solution and 38 times 1 μL of the HS solution was injected into the sample cell at 25 °C. Data were analyzed using the ITC_{200} microcal software.

Stability Studies. Analysis of proteolytic stabilities of the bicyclic peptides was performed by mixing 1.0 mg/mL solutions of the peptide in PBS, containing 100 μg/mL of umbelliferone (Sigma, Aldrich) as an internal standard, with equal volumes (1:1) of commercial human serum (Sigma, Aldrich) and incubating the samples at 37 °C. At certain time intervals (1, 2, 4, 8, 16, 32 h), a 50 μL sample was taken from the solution, mixed with 100 μL of a 10% solution of trifluoroacetic acid (TFA) in water (to precipitate serum proteins), centrifuged for 4 min at 13 000 rpm, and subsequently analyzed by UPLC/MS (Acquity, Waters) to quantify the amount of remaining peptide by peak integration. Peak areas were quantified using the internal standard umbelliferone and normalized to values determined at t = 0 s.

Statistics. To compare the uptake efficiency between experiments, the median fluorescent intensities of the tested peptides were normalized to nonaarginine (100%). Statistical analyses were performed with Graphpad Prism. In order to compare the significance of differences between peptides of one group, one-way analyses of variance (Anova) ($p < 0.05$) were performed, followed by a Bonferroni correction involving all pairs of comparison. The significance of differences between the bicyclic and the linear variants was tested using unpaired t tests. Since in each experiment all uptake efficiencies were normalized to the uptake of nonaarginine, for some figures, median values for peptides tested in different experiments were averaged and combined in one figure.

■ ASSOCIATED CONTENT

Supporting Information

Statistical analyses, all microscopy images of peptides not shown in the main text, flow cytometry data of peptides at 20 μM, the results of the CA group, and the graphs of the ITC measurements. This material is available free of charge via the Internet at http://pubs.acs.org/.

■ AUTHOR INFORMATION

Corresponding Authors

*E-mail: r.brock@ncmls.ru.nl, Tel: +31-24-3666213.

*E-mail: p.timmerman@pepscan.com, Tel: +31 320 225300, Fax: +31 320 225301.

Notes

The authors declare no competing financial interest.

■ ACKNOWLEDGMENTS

W. P. R. V. was supported by funds of the Radboud University Medical Centre.

■ ABBREVIATIONS

CPP, cell-penetrating peptide; HS, heparan sulfate; ITC, isothermal titration calorimetry

■ REFERENCES

(1) van den Berg, A., and Dowdy, S. F. (2011) Protein transduction domain delivery of therapeutic macromolecules. *Curr. Opin. Biotechnol. 22*, 888−93.

(2) Milletti, F. (2012) Cell-penetrating peptides: classes, origin, and current landscape. *Drug Discovery Today 17*, 850−60.

(3) Vives, E., Brodin, P., and Lebleu, B. (1997) A truncated HIV-1 Tat protein basic domain rapidly translocates through the plasma membrane and accumulates in the cell nucleus. *J. Biol. Chem. 272*, 16010−16017.

(4) Futaki, S., Suzuki, T., Ohashi, W., Yagami, T., Tanaka, S., Ueda, K., and Sugiura, Y. (2001) Arginine-rich peptides. An abundant source of membrane-permeable peptides having potential as carriers for intracellular protein delivery. *J. Biol. Chem. 276*, 5836−5840.

(5) Wender, P. A., Mitchell, D. J., Pattabiraman, K., Pelkey, E. T., Steinman, L., and Rothbard, J. B. (2000) The design, synthesis, and evaluation of molecules that enable or enhance cellular uptake: Peptoid molecular transporters. *Proc. Natl. Acad. Sci. U.S.A. 97*, 13003−13008.

(6) Sakai, N., Takeuchi, T., Futaki, S., and Matile, S. (2005) Direct observation of anion-mediated translocation of fluorescent oligoarginine carriers into and across bulk liquid and anionic bilayer membranes. *ChemBioChem 6*, 114−22.

(7) Jiao, C. Y., Delaroche, D., Burlina, F., Alves, I. D., Chassaing, G., and Sagan, S. (2009) Translocation and endocytosis for cell-penetrating peptide internalization. *J. Biol. Chem. 284*, 33957−65.

(8) Verdurmen, W. P., Thanos, M., Ruttekolk, I. R., Gulbins, E., and Brock, R. (2010) Cationic cell-penetrating peptides induce ceramide formation via acid sphingomyelinase: implications for uptake. *J. Controlled Release 147*, 171−9.

(9) Tunnemann, G., Martin, R. M., Haupt, S., Patsch, C., Edenhofer, F., and Cardoso, M. C. (2006) Cargo-dependent mode of uptake and bioavailability of TAT-containing proteins and peptides in living cells. *FASEB J. 20*, 1775−1784.

(10) Duchardt, F., Ruttekolk, I. R., Verdurmen, W. P., Lortat-Jacob, H., Burck, J., Hufnagel, H., Fischer, R., van den Heuvel, M., Lowik, D. W., Vuister, G. W., Ulrich, A., de Waard, M., and Brock, R. (2009) A cell-penetrating peptide derived from human lactoferrin with conformation-dependent uptake efficiency. *J. Biol. Chem. 284*, 36099−108.
(11) Alves, I. D., Bechara, C., Walrant, A., Zaltsman, Y., Jiao, C. Y., and Sagan, S. (2011) Relationships between membrane binding, affinity and cell internalization efficacy of a cell-penetrating peptide: penetratin as a case study. *PloS One 6*, e24096.
(12) Nakase, I., Tadokoro, A., Kawabata, N., Takeuchi, T., Katoh, H., Hiramoto, K., Negishi, M., Nomizu, M., Sugiura, Y., and Futaki, S. (2007) Interaction of arginine-rich peptides with membrane-associated proteoglycans is crucial for induction of actin organization and macropinocytosis. *Biochemistry 46*, 492−501.
(13) Richard, J. P., Melikov, K., Brooks, H., Prevot, P., Lebleu, B., and Chernomordik, L. V. (2005) Cellular uptake of unconjugated TAT peptide involves clathrin-dependent endocytosis and heparan sulfate receptors. *J. Biol. Chem. 280*, 15300−6.
(14) Wallbrecher, R., Verdurmen, W. P., Schmidt, S., Bovee-Geurts, P. H., Broecker, F., Reinhardt, A., van Kuppevelt, T. H., Seeberger, P. H., and Brock, R. The stoichiometry of peptide-heparan sulfate binding as a determinant of uptake efficiency of cell-penetrating peptides, *Cell. Mol. Life Sci.* 2013, DOI: 10.1007/s00018-013-1517-8 .
(15) Verdurmen, W. P., Bovee-Geurts, P. H., Wadhwani, P., Ulrich, A. S., Hallbrink, M., van Kuppevelt, T. H., and Brock, R. (2011) Preferential uptake of L- versus D-amino acid cell-penetrating peptides in a cell type-dependent manner. *Chem. Biol. 18*, 1000−10.
(16) Favretto, M. E., Wallbrecher, R., Schmidt, S., van de Putte, R., and Brock, R. Glycosaminoglycans in the cellular uptake of drug delivery vectors - Bystanders or active players? *J. Controlled Release* 2014, DOI: 10.1016/j.jconrel.2014.02.011.
(17) Wender, P. A., Mitchell, D. J., Pattabiraman, K., Pelkey, E. T., Steinman, L., and Rothbard, J. B. (2000) The design, synthesis, and evaluation of molecules that enable or enhance cellular uptake: peptoid molecular transporters. *Proc. Natl. Acad. Sci. U.S.A. 97*, 13003−8.
(18) Lattig-Tunnemann, G., Prinz, M., Hoffmann, D., Behlke, J., Palm-Apergi, C., Morano, I., Herce, H. D., and Cardoso, M. C. (2011) Backbone rigidity and static presentation of guanidinium groups increases cellular uptake of arginine-rich cell-penetrating peptides. *Nat. Commun. 2*, 453.
(19) Boisseau, S., Mabrouk, K., Ram, N., Garmy, N., Collin, V., Tadmouri, A., Mikati, M., Sabatier, J. M., Ronjat, M., Fantini, J., and De Waard, M. (2006) Cell penetration properties of maurocalcine, a natural venom peptide active on the intracellular ryanodine receptor. *Biochim. Biophys. Acta 1758*, 308−19.
(20) Kerkis, A., Kerkis, I., Radis-Baptista, G., Oliveira, E. B., Vianna-Morgante, A. M., Pereira, L. V., and Yamane, T. (2004) Crotamine is a novel cell-penetrating protein from the venom of rattlesnake Crotalus durissus terrificus. *Faseb J. 18*, 1407−9.
(21) Altafaj, X., Cheng, W., Esteve, E., Urbani, J., Grunwald, D., Sabatier, J. M., Coronado, R., De Waard, M., and Ronjat, M. (2005) Maurocalcine and domain A of the II-III loop of the dihydropyridine receptor Cav 1.1 subunit share common binding sites on the skeletal ryanodine receptor. *J. Biol. Chem. 280*, 4013−6.
(22) Timmerman, P., Beld, J., Puijk, W. C., and Meloen, R. H. (2005) Rapid and quantitative cyclization of multiple peptide loops onto synthetic scaffolds for structural mimicry of protein surfaces. *ChemBioChem 6*, 821−4.
(23) Heinis, C., Rutherford, T., Freund, S., and Winter, G. (2009) Phage-encoded combinatorial chemical libraries based on bicyclic peptides. *Nat. Chem. Biol. 5*, 502−7.
(24) Duchardt, F., Fotin-Mleczek, M., Schwarz, H., Fischer, R., and Brock, R. (2007) A comprehensive model for the endocytic uptake of cationic cell-penetrating peptides. *Traffic 8*, 848−866.
(25) van Asbeck, A. H., Beyerle, A., McNeill, H., Bovee-Geurts, P. H., Lindberg, S., Verdurmen, W. P., Hallbrink, M., Langel, U., Heidenreich, O., and Brock, R. (2013) Molecular parameters of siRNA-cell penetrating peptide nanocomplexes for efficient cellular delivery. *ACS Nano 7*, 3797−807.
(26) Ruttekolk, I. R., Witsenburg, J. J., Glauner, H., Bovee-Geurts, P. H., Ferro, E. S., Verdurmen, W. P., and Brock, R. (2012) The intracellular pharmacokinetics of terminally capped peptides. *Mol. Pharm. 9*, 1077−86.
(27) Molloy, S. S., Bresnahan, P. A., Leppla, S. H., Klimpel, K. R., and Thomas, G. (1992) Human furin is a calcium-dependent serine endoprotease that recognizes the sequence Arg-X-X-Arg and efficiently cleaves anthrax toxin protective antigen. *J. Biol. Chem. 267*, 16396−402.
(28) Walker, J. A., Molloy, S. S., Thomas, G., Sakaguchi, T., Yoshida, T., Chambers, T. M., and Kawaoka, Y. (1994) Sequence specificity of furin, a proprotein-processing endoprotease, for the hemagglutinin of a virulent avian influenza virus. *J. Virol. 68*, 1213−8.
(29) Benns, J. M., Choi, J. S., Mahato, R. I., Park, J. S., and Kim, S. W. (2000) pH-sensitive cationic polymer gene delivery vehicle: N-Ac-poly(L-histidine)-graft-poly(L-lysine) comb shaped polymer. *Bioconjugate Chem. 11*, 637−45.
(30) Hashemi, M., Parhiz, B. H., Hatefi, A., and Ramezani, M. (2011) Modified polyethyleneimine with histidine-lysine short peptides as gene carrier. *Cancer Gene Ther. 18*, 12−9.
(31) Lo, S. L., and Wang, S. (2008) An endosomolytic Tat peptide produced by incorporation of histidine and cysteine residues as a nonviral vector for DNA transfection. *Biomaterials 29*, 2408−14.
(32) Midoux, P., Pichon, C., Yaouanc, J. J., and Jaffres, P. A. (2009) Chemical vectors for gene delivery: a current review on polymers, peptides and lipids containing histidine or imidazole as nucleic acids carriers. *Br. J. Pharmacol. 157*, 166−78.
(33) Lecorche, P., Walrant, A., Burlina, F., Dutot, L., Sagan, S., Mallet, J. M., Desbat, B., Chassaing, G., Alves, I. D., and Lavielle, S. (2012) Cellular uptake and biophysical properties of galactose and/or tryptophan containing cell-penetrating peptides. *Biochim. Biophys. Acta 1818*, 448−57.
(34) Schibli, D. J., Epand, R. F., Vogel, H. J., and Epand, R. M. (2002) Tryptophan-rich antimicrobial peptides: comparative properties and membrane interactions. *Biochem. Cell Biol. 80*, 667−77.
(35) Fischer, R., Waizenegger, T., Kohler, K., and Brock, R. (2002) A quantitative validation of fluorophore-labelled cell-permeable peptide conjugates: fluorophore and cargo dependence of import. *Biochim. Biophys. Acta 1564*, 365−74.
(36) Brock, R. The uptake of arginine-rich cell-penetrating peptides: Putting the puzzle together, *Bioconjugate Chem.* 2014, DOI: 10.1021/bc500017t.
(37) Sarko, D., Beijer, B., Garcia Boy, R., Nothelfer, E. M., Leotta, K., Eisenhut, M., Altmann, A., Haberkorn, U., and Mier, W. (2010) The pharmacokinetics of cell-penetrating peptides. *Mol. Pharm. 7*, 2224−31.
(38) Jarver, P., Mager, I., and Langel, U. (2010) In vivo biodistribution and efficacy of peptide mediated delivery. *Trends Pharmacol. Sci. 31*, 528−535.
(39) Goncalves, E., Kitas, E., and Seelig, J. (2005) Binding of oligoarginine to membrane lipids and heparan sulfate: structural and thermodynamic characterization of a cell-penetrating peptide. *Biochemistry 44*, 2692−2702.
(40) Tyagi, M., Rusnati, M., Presta, M., and Giacca, M. (2001) Internalization of HIV-1 tat requires cell surface heparan sulfate proteoglycans. *J. Biol. Chem. 276*, 3254−3261.